Geothermal waters from the Taupo Volcanic Zone, New Zealand: Li, B and Sr isotopes characterization

Romain Millot, Aimee Hegan, Philippe Négrel

Geothermal waters from the Taupo Volcanic Zone, New Zealand: Li, B and Sr isotopes characterization

Romain Millot[1*], Aimee Hegan[1,2], Philippe Négrel[1]

(1) BRGM, Metrology Monitoring Analysis Department, Orléans, France

(2) School of Earth, Atmospheric and Environmental Sciences, the University of Manchester, Manchester, United Kingdom

[*] Corresponding author, e-mail: r.millot@brgm.fr

Abstract

In this study, we report chemical and isotope data for 23 geothermal water samples collected in New Zealand within the Taupo Volcanic Zone (TVZ). We analyzed major and trace elements including Li, B and Sr and their isotopic compositions (δ^7Li, δ^{11}B, ^{87}Sr/^{86}Sr) in high temperature geothermal waters collected from deep boreholes in different geothermal fields (Ohaaki, Wairakei, Mokai, Kawerau and Rotokawa geothermal systems). Lithium concentrations are high (from 4.5 to 19.9 mg/L) and lithium isotopic compositions (δ^7Li) are very homogeneous, being comprised between -0.5 and +1.4‰. In particular, it is noteworthy that, except the samples from the Kawerau geothermal field having slightly higher δ^7Li values (+1.4%), the other geothermal waters have a very constant δ^7Li signature around a mean value of 0‰ ± 0.6 (2σ, n=21). Boron concentrations are also high and relatively homogeneous for the geothermal samples, falling between 17.5 and 82.1 mg/L. Boron isotopic compositions (δ^{11}B) are all negative, and display a range between -6.7 and -1.9‰. These B isotope compositions are in agreement with those of the Ngawha geothermal field in New Zealand. Li and B isotope signatures are in a good agreement with a fluid signature mainly derived from water/rock interactions involving magmatic rocks with no evidence of seawater input. On the other hand, strontium concentrations are lower and more heterogeneous and fall between 2 and 165 µg/L. ^{87}Sr/^{86}Sr ratios range from 0.70549 to 0.70961. These Sr isotope compositions overlap those of the Rotorua geothermal field in New Zealand, also confirming that some geothermal waters (with more radiogenic strontium) have interacted with bedrocks from the metasedimentary basement. Each of these isotope systems on their own reveals important information about particular aspects of either water source or water/rock interaction processes, but, considered together, provide a more integrated understanding of the geothermal systems from the TVZ in New Zealand.

Keywords: Geothermal waters, New Zealand, Lithium isotopes, Boron isotopes, Strontium isotopes

5 102 words (without references and captions)

1. INTRODUCTION

In the present work, we report chemical and isotope data for 23 geothermal water samples from the Taupo Volcanic Zone (TVZ) in New Zealand. Chemical and isotope data were analyzed for these deep geothermal waters in order to provide further constraints on the characterization of the associated deep geothermal reservoirs. The present study aims therefore to characterize the fluids from the geothermal systems for the TVZ and, more specifically, to constrain the nature and origin of these fluids: two essential parameters for the characterization of a geothermal resource.

Major and trace elements are first investigated in order to determine the chemical signature of the TVZ geothermal samples. A multi-isotopic approach is then used to provide additional information for the characterization of these waters. Sr isotopes ($^{87}Sr/^{86}Sr$) are investigated in order to better constrain the signature of the reservoir the waters come from, given that Sr isotopes are a good tracer of water origin for groundwaters and geothermal waters (Négrel et al. 1997, Négrel 1999, Millot et al. 2007). In addition, we also determined Li and B isotopic compositions of the TVZ geothermal waters with the objective of evaluating the utility of these isotopic tools to constrain the water/rocks interactions. Indeed, the isotopic composition of boron ($\delta^{11}B$) is determined in an attempt to elucidate the source and process controlling B in geothermal waters (Aggarwal et al. 2003), and the use of Li isotopic systematics ($\delta^{7}Li$) is also explored, following recent papers indicating that Li isotopes seem to be an effective tracer of water/rock interactions in geothermal waters (Millot et al. 2007, Millot and Négrel 2007, Millot et al. 2010a).

One of the objectives of the present study is also to compare the different information that can be obtained using a multi-isotopic approach for the characterization of geothermal waters, more precisely, how the combination of these isotopic tracers could help in deciphering the water-rock interaction processes. However, it is important to keep in mind that each isotopic system can only provide information concerning the chemical behavior of the element, but considered together, this multi-isotope approach can provide a more integrated understanding of the TVZ geothermal system in New Zealand.

2. THE TAUPO VOLCANIC ZONE

Geothermal systems occur in many parts of New Zealand. The conventional geothermal resources of New Zealand are currently utilized to depths between 1 and 3 km, and temperatures up to 330°C. High temperature geothermal fields (T > 250°C) are principally located in the TVZ (Figure 1), with another high temperature field at Ngawha in Northland. Moderate to low and very low temperature systems (T < 250°C) are more widely scattered.

Some are associated with areas of young volcanism: in Northland, Hauraki Plains, and the coastal Bay of Plenty. Many hot springs, particularly in the South Island, are associated with faults and tectonic features. The TVZ is 20-80 km wide and extends from Mt Ruapehu in the south to the Okataina Volcanic Center in the north and continues 200 km offshore. The zone is flanked by thick aprons of welded pyroclastic flows that form shallow dipping plateaus.

Situated in the middle of the North Island of New Zealand, the TVZ is an area of both volcanic and geothermal activity. Rhyolitic volcanic activity in the area is thought to have commenced 1.6 Ma ago. The enhanced activity in the region is a result of an actively extending back-arc rift, due to the subduction of the Pacific plate beneath the North Island of New Zealand. This area is characterized by an extremely high heat flow. The average heat flux from the central zone of the TVZ, which contains most of the geothermal fields, is about 700 mW/m^2 (Bibby et al. 1995).

Within the TVZ, the different geothermal fields are distributed in two bands approximately 20 km apart. It was estimated by Bibby et al (1995), that 75% of the heat flow occurs in the eastern band and 25% in the west. Samples were collected from five geothermal fields within the TVZ: Kawerau, Rotokawa and Ohaaki from the eastern side, and Mokai and Wairakei from the western side (Figure 1).

Temperatures of over 300°C are found within the fluids of the geothermal systems within the TVZ, generally within the eastern fields e.g. Kawerau (315°C) and Rotokawa (330°C) (Kissling and Weir 2005). Maximum temperatures at Wairakei reach 265°C (Kissling and Weir 2005), with Mokai (326°C).

Giggenbach (1995) used the variations of H_2O, CO_2 and Cl in discharges from six geothermal systems within the TVZ to identify the existence of two distinct types of deep water supply. Falling along the eastern side of the TVZ: Kawerau, Ohaaki and Rotokawa display higher gas contents than the fields on the western side, including Mokai and Wairakei (illustrated by CO_2/Cl ratios above 3.9 ±1.5 vs. 0.14 ±0.1). According to Giggenbach (1995), the higher ratios were described as being of andesitic rock origin, with the lower ratios originating from rhyolitic material. The excess of volatiles present in fluid discharges from geothermal and volcanic systems along convergent plate boundaries are likely to be derived preferentially from the marine sedimentary fraction of subducted material (Giggenbach 1995).

The Mokai geothermal system lies 25 km northwest of Lake Taupo, and is thought to be 10 km^2, based on resistivity measurements (Kissling and Weir 2005).

The Rotokawa geothermal system lies 10 km northeast of Lake Taupo and has an area of 25 km^2, based on resistivity measurements (Hunt and Bowyer 2007, Heise et al. 2008). A mix of Paleozoic and Mesozoic greywackes form the basement of the system, with a mix of

ignimbrites and rhyolite lavas forming overlying layers, which are in turn covered by Holocene tuff (Krupp et al.1986, Wilson et al. 2007).

Hydrothermally altered greywacke sandstones dominate the basements at both the Kawerau and Ohaaki geothermal fields, however characterization by Wood et al. (2001) has shown that, despite similar lithologies, there are very different petrological characteristics between the two. As a result, the Ohaaki greywackes are analogous, for their bulk compositions, to granite, and the Kawerau greywackes to quartz diorite. The basement at Ohaaki also differs from those of the other fields due to the occurrence of (approx. 3%) argillite in fine partings (Wood et al. 2001).

In Table 1, the geothermal samples are listed with their origin (geothermal system), the borehole depth (m) and deep temperature (°C) estimated by chemical geothermometry.

3. ANALYTICAL METHODS

3.1. Major and trace elements

The samples were collected, after filtration and acidification on site, by MRP and Contact Energy, from the production pipeline using a fluid sampling separator. These geothermal sites are managed by Contact Energy Limited, the Tuaropaki Power Company, the Rotokawa Joint Venture and Mighty River Power Limited. All chemical analyses were performed in the BRGM laboratories using standard water analysis techniques such as Ion Chromatography (Cl), Inductively Coupled Plasma-Atomic Emission Spectroscopy (Li, B and Sr), Inductively Coupled Plasma-Mass Spectrometry (Ca and Mg), and Flame Emission Spectrometry (Na, K, Ca and SiO_2). Major species and trace elements were determined on conditioned samples, i.e., after filtration at 0.2 µm for the major anions, and after filtration at 0.2 µm and acidification with Suprapur HNO_3 acid (down to pH = 2) for the major cations and trace elements.

Accuracy and precision for major and trace elements was verified by repeated measurements of standard materials during the course of this study: namely Ion96-3 and LGC6020 for cations and anions and pure Li, B and Sr standard solutions (Merck). The accuracy of the major and trace element data is approx. ± 10%.

3.2. Lithium isotopes

Lithium isotopic compositions were measured using a Neptune Multi Collector ICP-MS (Thermo Fischer Scientific). $^{7}Li/^{6}Li$ ratios were normalized to the L-SVEC standard solution (NIST SRM 8545, Flesch et al. 1973) following the standard-sample bracketing method (see

Millot et al. 2004 for more details). The analytical protocol involves the acquisition of 15 ratios with 16 s integration time per ratio, and yields in-run precision better than 0.2‰ ($2\sigma_m$). Blank values are low, (i.e. 0.2%), and 5 minutes wash time is enough to reach a stable background value.

The samples were prepared beforehand with chemical separation/purification by ion chromatography in order to produce a pure mono-elemental solution. Chemical separation of Li from the matrix was achieved before the mass analysis using a cationic resin (a single column filled with 3 mL of BioRad AG® 50W-X12 resin, 200-400 mesh) and HCl acid media (0.2N) for 30 ng of Li. Blanks for the total chemical extraction were less than 30 pg of Li, which is negligible, since it represents a 10^{-3} blank/sample ratio.

Successful quantitative measurement of Li isotopic compositions requires 100% Li recovery. The column was, therefore, frequently calibrated and repeated analysis of the L-SVEC standard processed through columns shows 100% Li recovery and no induced isotope fractionation due to the purification process.

The accuracy and reproducibility of the entire method (purification procedure + mass analysis) were tested by repeated measurement of a seawater sample (IRMM BCR-403) after separation of Li from the matrix, for which we obtained a mean value of δ^7Li = +30.9‰ ± 0.3 (2σ, n=7) over the analysis period. This mean value is in good agreement with our long-term measurement (δ^7Li = +31.0‰ ± 0.5, 2σ, n=30, Millot et al. 2004) and with other values reported in the literature (see, for example, Millot et al. 2004 for a compilation with δ^7Li values for seawater ranging from +28.9 to 33.9‰). Consequently, based on long-term measurements of a seawater standard, we estimate the external reproducibility of our method to be around ± 0.5‰ (2σ).

3.3. Boron isotopes

Boron isotopic compositions were determined on a Finnigan MAT 261 solid source mass spectrometer in a dynamic mode. B isotope compositions were determined on conditioned samples (after filtration at 0.2 µm). For these samples, water volumes corresponding to a mass of 4 µg of B was processed using a two-step chemical purification through Amberlite IRA-743 selective resin. The boron aliquot sample (2 µg) was then loaded onto a Ta single filament with graphite, mannitol and Cs, and the B isotopes were determined by measuring the $Cs_2BO_2^+$ ion. The total boron blank is less than 10 ng. The values are given using the δ-notation (expressed in ‰) relative to the NBS951 boric acid standard. The $^{11}B/^{10}B$ of replicate analyses of the NBS951 boric acid standard after oxygen correction was 4.05122 ± 0.00122

183 (2σ, n=27) during this period. The reproducibility of the $\delta^{11}B$ determination is ± 0.3‰ (2σ) and
184 the internal uncertainty is better than 0.3‰ ($2\sigma_m$).
185 The accuracy and reproducibility of the whole procedure were verified by the repeated
186 measurements of the IAEA-B1 seawater standard (Gonfiantini et al. 2003) for which the
187 mean $\delta^{11}B$ value obtained is +39.22‰ ± 0.32 (2σ, n=33), in agreement with the accepted
188 value for seawater ($\delta^{11}B$ = +39.5‰, see data compilation reported by Aggarwal et al. 2004).
189
190 **3.4. Strontium isotopes**
191
192 Chemical purification of Sr (~3 µg) was performed using an ion-exchange column (Sr-Spec)
193 before mass analysis according to a method adapted from Pin and Bassin (1992), with total
194 blank <1 ng for the entire chemical procedure. After chemical separation, around 150 ng of
195 Sr was loaded onto a tungsten filament with tantalum activator and analysed with a Finnigan
196 MAT 262 multi-collector mass spectrometer. The $^{87}Sr/^{86}Sr$ ratios were normalized to an
197 $^{86}Sr/^{88}Sr$ ratio of 0.1194. An average internal precision of ± 10^{-5} ($2\sigma_m$) was obtained and the
198 reproducibility of the $^{87}Sr/^{86}Sr$ ratio measurements was tested by repeated analyses of the
199 NBS987 standard, for which we obtained a mean value of 0.710243 ± 0.000010 (2σ, n=9)
200 during the period of analysis.
201
202 **3.5. Chemical geothermometry**
203
204 The concentrations of most dissolved elements in geothermal waters depend on the
205 groundwater temperature and the weathered mineralogical assemblage (White 1965, Ellis
206 1970, Truesdell 1976, Arnórsson et al. 1983, Fouillac 1983). Since concentrations can be
207 controlled by temperature-dependent reactions, they could theoretically be used as
208 geothermometers to estimate the deep temperature of the water. In the present study, deep
209 temperature estimates were calculated based on SiO_2 concentrations following silica
210 geothermometer based on quartz, chalcedony, α or β cristobalite and amorphous silica
211 solubility (Fournier and Rowe 1966, Helgeson et al. 1978, Arnorsson et al. 1983). These
212 temperature estimates agree well with downhole measurements and with previous data
213 reported in the literature (Hedenquist 1990, Christenson et al. 2002).
214
215 **4. RESULTS AND COMMENTS**
216
217 **4.1. Major and trace elements**
218

Geothermal waters are commonly characterized by examining the behavior of the major elements (Table 1). In this context, Figure 2 illustrates the relationship between Cl, considered as a conservative element, and Na, which is largely controlled by water/rock interactions. Whereas Cl concentrations range between 666 and 2834 mg/L, Na concentrations range between 388 and 1477 mg/L. From a general point of view, we observe a good relationship between Na and Cl (Figure 2), indicating that the geothermal waters display a large range of salinity, with Na and Cl concentrations increasing from Rotokawa, Kawerau, Ohaaki, and Wairakei up to the samples from Mokai.

Other major elements range from 72 to 338 mg/L for K, from 0.005 to 0.028 mg/L for Mg, and from 0.1 to 27.7 mg/L for Ca. Anions concentrations range between 2.6 and 74.8 mg/L for SO_4 and between 1.1 and 5.9 mg/L for Br. Silica concentrations are high, ranging from 384 to 1169 mg/L.

Concerning trace elements, and those of interest for the present work: Li concentrations are high, ranging from 4.5 to 19.9 mg/L. B concentrations are also high, ranging between 17.5 and 82.1 mg/L (BR49, Ohaaki). If we exclude the sample with the highest concentration, B contents are homogeneous, falling between 17.5 and 42.3 mg/L. Finally, Sr concentrations are clearly lower, ranging from 0.002 to 0.165 mg/L. The lithium, boron and strontium concentrations are in agreement with the data reported in the literature for worldwide geothermal waters (Mossadik 1997, Williams et al. 2001, Aggarwal et al. 2003, Millot et al. 2007, Millot and Négrel 2007, Millot et al. 2009, Millot et al. 2010a).

Because Na is mainly controlled by water/rock interactions, it is interesting to also investigate the relationships between Na and Li, B and Sr (Figure 3). Firstly, it can be observed (Figure 3a), that all the geothermal waters define a general positive relationship between Na and Li, which suggests that, like Na, Li is mainly controlled by water/rock interactions. Secondly and by contrast, when B concentrations are plotted against Na (Figure 3b), different trends emerge. Indeed, we can observe different positive correlations between B and Na, meaning that B is also controlled by water/rock interactions, but there is not a single general trend at the scale of the whole TVZ as observed for Li. From that graph (Figure 3b) geothermal samples can be divided into different groups of samples: thus, the geothermal waters from Kawerau and Rotokawa seem to define a single trend, those from Ohaaki are different, and finally, those from Mokai and Wairakei seem to also plot on a single trend. These trends correlate with the spatial distribution of geothermal fields within the TVZ. The geothermal systems from Mokai and Wairakei are located in the western side of the TVZ, and those form Kawerau, Rotokawa and Ohaaki are located in the eastern side of the TVZ. Finally, when Sr concentrations are plotted as a function of Na (Figure 3c), it seems that there is no global link between these two elements, except that the geothermal waters from Kawerau and Rotokawa show a positive relationship.

Additional information can also be obtained when the concentrations of trace elements are plotted as a function of the deep temperature of the water calculated by chemical geothermometry (Figure 4). Both Li and B concentrations appear to be relatively constant and independent of the temperature of the fluid. On the other hand, Sr concentrations appear to be anti-correlated with the temperature of the fluid (Figure 4b). Such a feature strongly suggests that dilution is occurring in the system by mixing of shallower and colder waters. However, it is also likely that the lower Sr contents can also be controlled by calcite precipitation. Finally, in Figure 4d, SiO_2 concentrations and deep temperature show a strong correlation (R^2 = 0.84) but this is an induced correlation, due to the fact that, deep temperature estimates were calculated based on SiO_2 concentrations following silica geothermometers.

4.2. Li-B-Sr isotopes

Li isotopes are reported in Table 1 and lithium isotopic compositions (δ^7Li, ‰) are very homogeneous. For all the samples, the range of variation for δ^7Li values is small (1.9‰ in total) ranging between -0.52 and +1.42‰, respectively, for sample BR9 (Ohaaki) and KA37 (Kawerau). Omitting the two samples from Kawerau, which have slightly higher δ^7Li values (+1.42 and +1.38%), the other geothermal waters have a very constant δ^7Li signature around a mean value of 0‰ ± 0.6 (2σ, n=21). This small range of variation (± 0.6‰) is almost the same as our external reproducibility of our method for Li isotopes analysis (± 0.5‰, 2σ, section 3.2.). This result means that lithium has either the same origin in these fluids and/or the process(es) that control Li isotope fractionation is (are) the same for all the geothermal water samples under consideration. Compared to scarce literature data for geothermal waters (Millot and Négrel 2007, Millot et al. 2007, 2009, 2010), geothermal waters from the TVZ display low δ^7Li values.

B isotopes are also reported in Table 1. The range of δ^{11}B values is of 4.8‰ in total, from -6.70‰ (RK14, Rotokawa) to -1.92‰ (WK235, Wairakei). A plot of B isotopes (δ^{11}B, ‰) as a function of B concentrations (Figure 5b) shows that, with the exception of sample BR49 (Ohaaki) having the highest B concentrations, there is no large variation of both B isotopes and concentrations. However, Rotokawa and Ohaaki geothermal waters have the lowest δ^{11}B values, and, by contrast, geothermal waters from Wairakei, Mokai and Kawerau have the highest δ^{11}B values. Geothermal samples from this study can be compared with literature data from the Ngawha geothermal field (Aggarwal et al. 2003) for B isotopes. The Ngawha geothermal field is the only high temperature geothermal field in New Zealand that is located outside the TVZ. It is located on the central axis of the Northland peninsula in a Quaternary–

Holocene basaltic field (Kaikohe volcanic field). Measurements of water samples from the Ngawha geothermal system fall within a limited range of $\delta^{11}B$ values between -3.9 and -3.1‰, overlapping the TVZ data.

Sr isotopes are also reported in Table 1. $^{87}Sr/^{86}Sr$ ratios range from 0.70549 (WK245, Wairakei) to 0.70961 (BR49, Ohaaki). Sr isotopes are plotted as a function of Sr concentrations in Figure 5c and show no general trend or any relationship with the spatial distribution of the samples (eastern vs. western location). However, it is noteworthy that geothermal waters from the Wairakei field display the most constant $^{87}Sr/^{86}Sr$ ratios, between 0.70549 and 0.70574. Sr isotope data reported here are in agreement with those of Graham (1992) for the Rotorua geothermal waters (0.70514-0.70791) and for the Ohaaki geothermal field site (0.70746, Grimes et al. 2000) also located in New Zealand.

5. DISCUSSION

Collectively, the lithium, boron and strontium isotopes can be used to identify the different sources contributing to the Li-B-Sr isotopic signature and to determine the main processes controlling these elements and their isotopes in the geothermal waters of the TVZ.

First, Sr isotopes are investigated in the present work in order to better define the signature of the reservoir the geothermal waters came from, given that Sr isotopes are a good tracer of water origin for groundwaters and geothermal waters (Goldstein and Jacobsen 1987, Négrel et al. 1997, Négrel 1999, Négrel et al. 2000). Second, lithium and boron isotopic compositions ($\delta^{7}Li$ and $\delta^{11}B$) are also considered in order to provide further constraints on the origin of Li and B in these geothermal waters.

As already mentioned, Sr isotopes display a large range in the geothermal waters of the TVZ (from 0.70549 to 0.70961). In addition, we also observed in the previous section that if dilution processes happen in the system (by shallow, colder waters), it could probably explain the distribution of Sr concentrations. On the other hand, the higher $^{87}Sr/^{86}Sr$ ratios in geothermal waters are close to the value of modern seawater ($^{87}Sr/^{86}Sr$ = 0.70917, Dia et al. 1992). Collectively, these observations could reflect dilution of geothermal waters by seawater (cold and shallow water input with high Sr isotopic ratio). A seawater mixing calculation is displayed in Figure 6, in which $^{87}Sr/^{86}Sr$ ratios are plotted vs. Cl/Sr ratios. The geothermal end member is chosen to be sample RK5 (Rotokawa), which has both the lowest $^{87}Sr/^{86}Sr$ and the highest Cl/Sr ratios, and is, thus, representative of geothermal waters being least affected by potential seawater contribution. No significant contribution of seawater for strontium is observed in the geothermal systems of the TVZ, it means that Sr and its isotopes are mainly controlled by the signature of the bedrocks themselves.

As already mentioned in section 2., the TVZ is an area of rhyolitic volcanic activity and hydrothermal altered sediments (greywackes) form the basement of the system. On the left side of Figure 6, we show the ranges of $^{87}Sr/^{86}Sr$ ratios for the bedrocks of the system: volcanic country rocks (rhyolite, ignimbrite and breccia, 0.7049-0.7057) reported by Graham (1992), basalts for the TVZ (0.7026-0.7052, Gamble et al. 1993) and metasedimentary basement rocks that have $^{87}Sr/^{86}Sr$ values between 0.705 for greywackes up to 0.725 for argilites (Graham 1992). Therefore it is likely that the most radiogenic Sr isotope ratios are the result of a significant contribution of waters having interacted with bedrocks having more radiogenic strontium like metasedimentary basement rocks.

Finally, when $^{87}Sr/^{86}Sr$ ratios of the TVZ fluids are compared to literature data for other geothermal fluids (Figure 7a), the geothermal waters from the TVZ are similar to those of Graham (1992) for the Rotorua geothermal waters in New Zealand (0.70514-0.70791), but are significantly different from those of Iceland, which have $^{87}Sr/^{86}Sr$ ratios ranging between 0.7032 and 0.7042 (Millot et al. 2009). However, all of the geothermal waters display a similar range for Cl/Sr ratios, except for those of the Rotokawa geothermal field, which have higher Cl/Sr ratios. It is very likely that the significant difference in the Sr isotopes signature between the geothermal systems from New Zealand and those from Iceland is related to the signature of the volcanic basement rocks. New Zealand volcanic activity commenced 1.6 Ma ago, allowing in-growth of radiogenic Sr from Rb, whereas the geothermal systems in Iceland are located in the central volcanic area, which is only < 0.8 Ma old.

Boron isotopes ($\delta^{11}B$) range from -6.70‰ to -1.92‰ in the geothermal waters from the TVZ, these values are in a good agreement with a volcanic origin of the waters (< 0‰: Barth 1993, 2000). In addition, according to Aggarwal et al. (2003) for the Ngawha geothermal field, the relatively low $\delta^{11}B$ values for the fluids implies no significant marine input into the geothermal reservoir and this is also in accord with other geochemical data, e.g. average Cl/B = 53 compared to seawater Cl/B = 4839. In Figure 7b, it is important to note that the worldwide geothermal waters have a $\delta^{11}B$ signature almost entirely comprised between -10 and 0‰, with the exception of the samples from Reykjanes and Svartsengi geothermal fields in Iceland, for which the contribution of seawater is significant (Millot et al. 2009). And, like the Na concentration (Figure 3), the Cl/B is also variable according to the location of the geothermal field.

Lithium isotopic compositions ($\delta^{7}Li$, ‰) are very homogeneous for the geothermal waters of the TVZ. In Figure 7c, we can compare Li isotope data for TVZ geothermal waters with geothermal waters from Iceland (Millot et al. 2009) and with geothermal systems from the Guadeloupe and Martinique islands (volcanic islands belonging to the Lesser Antilles arc, French West Indies, Millot et al. 2010a). The geothermal waters from the TVZ are distinct

from those of other geothermal systems. Indeed, the geothermal waters from the TVZ display the lowest δ^7Li yet reported for geothermal waters, but they also have the lowest Cl/Li ratios. In addition, whereas the geothermal fields from Iceland and French West Indies can have a significant contribution of Li from seawater (Millot et al. 2009, 2010b), it is obvious that seawater has no influence on the composition of the geothermal waters from New-Zealand.

Several studies of Li-isotope behaviour in near-surface environments have shown that δ^7Li values do not directly reflect the signature of the bedrock, but instead are controlled by fractionation during water/rock interactions during the formation of secondary minerals of alteration (Huh et al. 1998, 2001, 2004, Pistiner and Henderson 2003, Rudnick et al. 2004, Kisakürek et al. 2004, 2005, Pogge von Strandmann et al. 2006, Vigier et al. 2009, Teng et al. 2010, Lemarchand et al. 2010, Millot et al. 2010b). And it has been suggested that the δ^7Li signature in the liquid might be controlled by the preferential retention of light lithium isotope (^{6}Li) into secondary mineral phases during the weathering processes. It has also been shown that the fractionation of lithium isotopes during water/rock interactions also depends on temperature because different secondary minerals might control the uptake or release of lithium in secondary minerals depending on the temperature of interaction and the associated dissolution/precipitation reaction (Chan and Edmond 1988, Chan et al. 1992; 1993; 1994; Chan et al. 2002). All geothermal fluids from the TVZ show homogeneous and low δ^7Li values, indicating that temperature is probably not the main factor in controlling the Li isotopic composition of the geothermal fluids. Rather, it is more likely that the consistent low δ^7Li values in these geothermal fluids could reflect Li leaching from the same source rock. When plotted on isotope vs. isotope diagrams (Figure 8), the following conclusions can be reached: i) Li isotope signatures are very homogeneous and do not allow the discrimination of any geothermal field, suggesting that the fluids are well-mixed for Li and that it is the process of water/rock interaction at high temperature that is the main factor that determine both Li and its isotopes distribution in geothermal waters of the TVZ; ii) B isotopes are less homogeneous, and some differences could exist between the geothermal fields; although B and its isotopes are also mainly controlled by water/rock interaction processes, there is a small difference for δ^{11}B values between geothermal waters from Rotokawa and Ohaaki on the one hand and those from Mokai, Wairakei and Kawerau on the other hand; iii) the Sr isotopes signatures vary widely and confirm distinction between waters from different locations. From a general point of view, the geographical distribution of the samples within the TVZ (eastern vs. western location) shows that it could affect B and Sr but not Li isotopes, meaning that it is likely that the fluids are well-mixed for Li and less for B and Sr. In addition, for Sr isotopes, the isotopic signal also depends on the type of basement rocks.

6. CONCLUSIONS

The main conclusions of the Li-B-Sr isotopes characterization of the geothermal waters from the Taupo Volcanic Zone are:

• Lithium concentrations are high (ranging from 4.5 to 19.9 mg/L) and lithium isotopic compositions (δ^7Li) are homogeneous ranging between -0.5 and +1.4‰. Li isotope tracing shows that the input of seawater is negligible in these geothermal waters and that Li and its isotopes are mainly controlled by equilibrium exchange with magmatic rocks at high temperature.

• Boron concentrations are also high (17.5 and 82.1 mg/L) and relatively homogeneous and boron isotopic compositions (δ^{11}B) are all negative, ranging from -6.7 to -1.9‰. This B isotope signature is in a good agreement with a fluid signature derived mainly from water/rock interactions involving magmatic rocks and no seawater input.

• Strontium concentrations (0.02 to 0.165 mg/L) are lower and more heterogeneous while ^{87}Sr/^{86}Sr ratios range between 0.70549 and 0.70961. These Sr isotope compositions are similar to those of local magmatic bedrocks and the highest Sr isotope ratios are the result of a significant contribution of waters having interacted with bedrocks having more radiogenic strontium like, metasedimentary basement rocks.

Each of these isotope systems on their own reveals important information about particular aspects of either water source or water/rock interaction processes, but, considered together, provide a more integrated understanding of the geothermal systems from the TVZ in New Zealand. However, the combination of Li, B and Sr isotopic systems highlights the complexity of the study of these geothermal waters, and the use of only one isotopic tool could lead to an incomplete characterization of the geothermal waters.

Acknowledgements

This work was funded by the Research Division of the BRGM. This work benefited from the collaboration of BRGM Chemistry laboratories for the major and trace elemental analyses: J.P. Ghestem, T. Conte and C. Crouzet are thanked for their help, as well as M. Robert for her help in the Neptune laboratory. C. Guerrot (TIMS analytic sector, BRGM) is acknowledged for B and Sr isotope data. We cordially thank Contact Energy Limited, the Tuaropaki Power Company, the Rotokawa Joint Venture and Mighty River Power Limited for providing the samples. Ed Mroczek (GNS Science) and Tom Powell (Mighty River Power Limited) are acknowledged for critical comments. E. Petelet-Giraud is also thanked for fruitful discussions. A. Hegan was supported by a fellowship from AquaTRAIN MRTN (Contract No. MRTN-CT-2006-035420) funded by the European Commission FP6 Marie Curie Actions - Human Resources and Mobility Activity Area, Research Training Networks. RM is particularly grateful to C. Fouillac for the opportunity to work on this subject. R. Rudnick and an anonymous reviewer are acknowledged for providing helpful reviews of this manuscript. L. Aquilina is also thanked for editorial handling and constructive comments. This is BRGM contribution n° XXXX.

References

Aggarwal J.K., Sheppard D., Mezger K., Pernicka E. (2003) Precise and accurate determination of boron isotope ratios by multiple collector ICP-MS: origin of boron in the Ngawha geothermal system, New Zealand. Chemical Geology, 199: 331-342.

Aggarwal J.K., Mezger K., Pernicka E., Meixner A. (2004) The effect of instrumental mass bias on $\delta^{11}B$ measurements: a comparison between thermal ionisation mass spectrometry and multiple-collector ICP-MS. International Journal of Mass Spectrometry, 232: 259-263.

Arnórsson S., Gunnlaugsson E., Svavarsson H. (1983) The geochemistry of geothermal waters in Iceland. III. Chemical geothermometry in geothermal investigations. Geochimica Cosmochimica Acta, 47: 567-577.

Barth S.R. (1993) Boron isotope variations in nature: a synthesis. Geologische Rundschau, 82: 640-641.

Barth S.R. (2000) Geochemical and boron, oxygen and hydrogen isotopic constraints on the origin of salinity in groundwaters from the crystalline basement of the Alpine Foreland. Applied Geochemistry, 15: 937-952.

Bibby H.M., Caldwell T.G., Davey F.J., Webb T.H. (1995) Geophysical evidence on the structure of the Taupo volcanic zone and its hydrothermal circulation. Journal of Volcanology and Geothermal Research, 68: 29-58.

Chan L.H. and Edmond J.M. (1988) Variation of lithium isotope composition in the marine environment: A preliminary report. Geochimica et Cosmochimica Acta, 52, 1711-1717.

Chan L.H., Edmond J.M., Thompson G., Gillis K. (1992) Lithium isotopic composition of submarine basalts: implications for the lithium cycle in the oceans. Earth and Planetary Science Letters, 108, 151-160.

Chan L.H., Edmond J.M., Thompson G. (1993) A lithium isotope study of hot springs and metabasalts from mid-ocean ridge hydrothermal systems. Journal of Geophysical Research, 98, 9653-9659.

Chan L.H., Gieskes J.M., You C.F., Edmond J.M. (1994) Lithium isotope geochemistry of sediments and hydrothermal fluids of the Guaymas Basin, Gulf of California. Geochimica et Cosmochimica Acta, 58, 4443-4454.

Christenson B.W., Mroczek E.K., Kennedy B.M., van Soest M.C., Stewart M.K., Lyon G. (2002) Ohaaki reservoir chemistry: characteristics of an arc-type hydrothermal system in the Taupo Volcanic Zone, New Zealand. Journal of Volcanology and Geothermal Research, 115: 53-82.

481 Chan L. H., Alt J.C., Teagle D.A.H. (2002) Lithium and lithium isotope profiles through the
482 upper oceanic crust: a study of seawater-basalt exchange at ODP Sites 504B and 896A.
483 Earth and Planetary Science Letters, 201, 187-201.
484 Dia A.N., Cohen A.S., O'Nions R.K., Shackleton N.J. (1992) Seawater Sr isotope variation
485 over the past 300 kyr and influence of global climate cycles. Nature, 356: 786-788.
486 Ellis A. J. (1970) Quantitative interpretations of chemical characteristics of hydrothermal
487 systems. Geothermics Special Issue, 2: 516-528.
488 Flesch G.D., Anderson A.R., Svec H.J. (1973) A secondary isotopic standard for $^{6}Li/^{7}Li$
489 determinations. International Journal of Mass Spectrometry and Ion Physics, 12: 265-
490 272.
491 Fouillac C. (1983) Chemical geothermometry in CO_2-rich thermal waters. Example of the
492 French Massif central. Geothermics, 12: 149-160.
493 Fournier R.O., Rowe J.J. (1966) Estimation of underground temperatures from the silica
494 content of water from hot springs and wet-steam wells. American Journal of Science,
495 264: 685-697.
496 Gamble J.A., Smith I.E.M., McCulloch M.T., Graham I.J., Kokelaar B.P. (1993) The
497 geochemistry and petrogenesis of basalts from the Taupo Volcanic Zone and Kermadec
498 Island Arc, S.W. Pacific. Journal of Volcanology and Geothermal Research, 54: 265-290.
499 Giggenbach W.F. (1995) Variations in the chemical and isotopic composition of fluids
500 discharged from the Taupo Volcanic Zone, New Zealand. Journal of Volcanology and
501 Geothermal Research, 68: 89-116.
502 Goldstein S.J., Jacobsen S.B. (1987) The Nd and Sr Isotopic systematics of river-water
503 dissolved material: implications for the sources of Nd and Sr in seawater. Chemical
504 Geology, 66: 245-272.
505 Gonfiantini R., Tonarini S., Gröning M., Adorni-Braccesi A., Al-Ammar A.S., Astner M.,
506 Bächler S., Barnes R.M., Bassett R.L., Cocherie A., Deyhle A., Dini A., Ferrara G.,
507 Gaillardet J., Grimm J., Guerrot C., Krähenbühl U., Layne G., Lemarchand D., Meixner
508 A., Northington D.J., Pennisi M., Reitznerová E., Rodushkin I., Sugiura N., Surberg R.,
509 Tonn S., Wiedenbeck M., Wunderli S., Xiao Y., Zack T. (2003) Intercomparison of boron
510 isotope and concentration measurements. Part II: Evaluation of results. Geostandards
511 Newsletter, 27: 41-57.
512 Graham I. J. (1992) Strontium isotope compositions of Rotorua geothermal waters.
513 Geothermics, 21: 165-180.
514 Grimes S., Rickard D., Hawkesworth C., van Calsteren P., Browne R. (2000) The
515 Broadlands–Ohaaki geothermal system, New Zealand Part 1. Strontium isotope
516 distribution in well BrO-29. Chemical Geology, 163: 247-265.

Hedenquist J.W. (1990) The thermal and geochemical structure of the Broadlands-Ohaaki geothermal system, New Zealand. Geothermics, 19: 151-185.

Heise W., Caldwell T.G., Bibby H.M., Bannister S.C. (2008) Three-dimensional modelling of magnetotelluric data from the Rotokawa geothermal field, Taupo Volcanic Zone, New Zealand. Geophysical Journal International, 173: 740-750.

Helgeson H.C., Delany J.M., Nesbitt H.W., Bird D.K. (1978) Summary and critique of the thermodynamic properties of rock-forming minerals. American Journal of Science, 278A.

Huh Y., Chan L.C., Zhang L., Edmond J.M. (1998) Lithium and its isotopes in major world rivers: implications for weathering and the oceanic budget. Geochimica et Cosmochimica Acta, 62: 2039-2051.

Huh Y., Chan L.C., Edmond J.M. (2001) Lithium isotopes as a probe of weathering processes: Orinoco River. Earth and Planetary Science Letters, 194: 189-199.

Huh Y., Chan L.C., Chadwick O.A. (2004) Behavior of lithium and its isotopes during weathering of Hawaiian basalt. Geochemistry, Geophysics, Geosystems, 5: 1-22.

Hunt T., Bowyer D. (2007) Reinjection and gravity changes at Rotokawa geothermal field, New Zealand. Geothermics, 36: 421-435.

Kisakürek B., Widdowson M., James R.H. (2004) Behaviour of Li isotopes during continental weathering: the Bidar laterite profile, India. Chemical Geology, 212: 27-44.

Kisakürek B., James R.H., Harris N.B.W. (2005) Li and δ^7Li in Himalayan rivers: Proxies for silicate weathering? Earth and Planetary Science Letters, 237: 387-401.

Kissling W.M., Weir G.J. (2005) The spatial distribution of the geothermal fields in the Taupo Volcanic Zone, New Zealand. Journal of Volcanology and Geothermal Research, 145: 136-150.

Krupp E., Browne P.R.L., Henley R.W., Seward T.M. (1986) Rotokawa Geothermal Field. In: R.W. Henley, J.W. Hedenquist and P.J. Roberts, Editors, Guide to the Active Epithermal (Geothermal) Systems and Precious Metal Deposits of New Zealand, Gebruder Borntraeger, Berlin, Stuttgart, pp. 47–55.

Lemarchand E., Chabaux F., Vigier N., Millot R., Pierret M.C. (2010) Lithium isotope systematics in a forested granitic catchment (Strengbach, Vosges Mountains, France). Geochimica et Cosmochimica Acta, 74: 4612-4628.

Millot R., Guerrot C., Vigier N. (2004) Accurate and high precision measurement of lithium isotopes in two reference materials by MC-ICP-MS. Geostandards and Geoanalytical Research, 28: 53-159.

Millot R., Négrel Ph. (2007) Multi-isotopic tracing (δ^7Li, δ^{11}B, ^{87}Sr/^{86}Sr) and chemical geothermometry: evidence from hydro-geothermal systems in France. Chemical Geology, 244: 664-678.

553 Millot R., Négrel Ph., Petelet-Giraud E. (2007) Multi-isotopic (Li, B, Sr, Nd) approach for
554 geothermal reservoir characterization in the Limagne Basin (Massif Central, France)
555 Applied Geochemistry, 22: 2307-2325.
556 Millot R., Asmundsson R., Négrel Ph., Sanjuan B., Bullen T.D. (2009) Multi-isotopic (H, O, C,
557 S, Li, B, Si, Sr, Nd) approach for geothermal fluid characterization in Iceland.
558 Goldschmidt Conference 2009, Davos, Switzerland.
559 Millot R., Scaillet B., Sanjuan B. (2010a) Lithium isotopes in island arc geothermal systems:
560 Guadeloupe, Martinique (French West Indies) and experimental approach. Geochimica
561 et Cosmochimica Acta, 74: 1852-1871.
562 Millot R., Vigier N., Gaillardet J. (2010b) Behaviour of lithium and its isotopes during
563 weathering in the Mackenzie Basin, Canada. Geochimica et Cosmochimica Acta, 74:
564 3897-3912.
565 Mossadik H. (1997) Les isotopes du bore, traceurs naturels dans les eaux. Mise au point de
566 l'analyse en spectrométrie de masse à source solide et application à différents
567 environnements. PhD Thesis, Université d'Orléans, Orléans.
568 Négrel Ph., Fouillac C. Brach M. (1997) Occurrence of mineral water springs in the stream
569 channel of the Allier River (Massif Central, France): chemical and Sr isotope constraints.
570 Journal of Hydrology, 203: 143-153.
571 Négrel Ph. (1999) Geochemical study in a granitic area, the Margeride, France: chemical
572 element behavior and 87Sr/86Sr constraints. Aquatic Geochemistry, 5: 125-165.
573 Négrel Ph., Guerrot C., Cocherie A., Azaroual M., Brach M., Fouillac C. (2000) Rare Earth
574 Elements, neodymium and strontium isotopic systematics in mineral waters: evidence
575 from the Massif Central, France. Applied Geochemistry, 15: 1345-1367.
576 Palmer M.R., Sturchio N.C. (1990) The boron isotope systematics of the Yellowstone
577 National Park (Wyoming) hydrothermal system: A reconnaissance. Geochimica et
578 Cosmochimica Acta, 54: 2811-2815.
579 Pin C., Bassin C. (1992) Evaluation of a strontium specific extraction chromatographic
580 method for isotopic analysis in geological materials. Analytica Chimica Acta, 269: 249-
581 255.
582 Pistiner J.S., Henderson G.M. (2003) Lithium isotope fractionation during continental
583 weathering processes. Earth and Planetary Science Letters, 214: 327-339.
584 Pogge von Strandmann P.A.E., Burton K.W., James R.H., van Calsteren P., Gislason S.R.,
585 Mokadem F. (2006) Riverine behaviour of uranium and lithium isotopes in an actively
586 glaciated basaltic terrain. Earth and Planetary Science Letters, 251: 134-147.
587 Rudnick R.L., Tomascak P.B., Njo H.B., Gardner L.R. (2004) Extreme lithium isotopic
588 fractionation during continental weathering revealed in saprolites from South Carolina.
589 Chemical Geology, 212: 45-57.

590 Teng F.Z., Li W.Y. Rudnick R.L., Gardner L.R. (2010) Contrasting lithium and magnesium
591 isotope fractionation during continental weathering. Earth and Planetary Science Letters,
592 300: 63-71.
593 Truesdell A.H. (1976) Geochemical techniques in exploration, summary of section III. Proc.
594 Sec. United Nations Symp. Develop. Use Geotherm. Res., San Francisco, 53-79.
595 Vigier N., Gislason S.R., Burton K.W., Millot R., Mokadem F. (2009) The relationship
596 between riverine lithium isotope composition and silicate weathering rates in Iceland.
597 Earth and Planetary Science Letters, 287: 434-441.
598 White D.E. (1965) Saline waters of sedimentary rocks. Fluids in Subsurface Environments -
599 A Symposium. Am. Ass. Petrol. Geol. Mem., 4: 342-366.
600 Williams L.B., Hervig R.L., Hutcheon I. (2001) Boron isotope geochemistry during diagenesis
601 Part II. Application to organic-rich sediments. Geochimica et Cosmochimica Acta, 65:
602 1783-1794.
603 Wilson N., Webster-Brown J., Brown K. (2007) Controls on stibnite precipitation at two New
604 Zealand geothermal power stations, Geothermics, 36: 330-347.
605 Wood C.P., Brathwaite R.L., Rosenberg M.D. (2001) Basement structure, lithology and
606 permeability at Kawerau and Ohaaki geothermal fields, New Zealand. Geothermics, 30 :
607 461-481.
608

Table caption

Table 1

Sample list including geothermal site, sample i.d., latitude and longitude coordinates, depth of borehole (m), deep temperature estimates given by geothermometry (°C) and date of sampling. Major and trace elements concentrations (mg/L) in the geothermal water samples are also reported in this table and Li, B and Sr isotopic compositions. d.l. is the detection limit (5 µg/L for Mg). Individual errors ($2\sigma_m$) are also reported for isotopic data.

Figure captions

Figure 1

Geothermal samples location. These geothermal waters were sampled by Contact Energy Limited for Ohaaki and Wairakei geothermal systems and by Mighty River Power Limited (MRP) for Mokai, Kawerau and Rotokawa geothermal systems respectively.

Figure 2

Cl concentrations (mg/L) plotted as a function of Na concentrations (mg/L).

Figure 3

Li, B and Sr concentrations (mg/L) plotted as a function of Na concentrations (mg/L). The dashed lines represent the 2σ uncertainty on the linear correlations.

Figure 4

Li, Sr, B and SiO_2 concentrations (mg/L) plotted as a function of the deep temperature (°C) estimated by geothermometry. Correlations have been added as well as a 2σ interval of confidence.

Figure 5

a: Li isotopes plotted as a function of Li concentrations (mg/L). The errors bars correspond to the external reproducibility of our method for Li isotopes analysis ± 0.5‰, 2σ.

b : B isotopes plotted as a function of B concentrations (mg/L). The errors bars correspond to the external reproducibility of our method for B isotopes analysis ± 0.3‰, 2σ.

c : Sr isotopes plotted as a function of Sr concentrations (mg/L). The errors bars are included within the sample symbol and correspond to the external reproducibility of our method for Sr isotopes analysis ± 0.000020, 2σ.

Figure 6

Sr isotopes plotted as a function of Cl/Sr massic ratio. Fields for volcanic country rocks, TVZ basalts and metasedimentary basement rocks have also been added, see text for comments.

Figure 7

a : Sr isotopes plotted as a function of Cl/Sr massic ratio. Comparison with geothermal waters from Rotorua geothermal system (Graham 1992) and geothermal systems from Iceland (Millot et al. 2009).

b : B isotopes plotted as a function of Cl/B massic ratio. Comparison with geothermal waters from Ngawha geothermal system (Graham 1992), Yellowstone (Palmer and Sturchio 1990) and geothermal systems from Iceland (Millot et al. 2009).

c : Li isotopes plotted as a function of Cl/Li massic ratio. Comparison with geothermal waters from Iceland (Millot et al. 2009) and from the Antilles (French West Indies, Millot et al. 2010a).

Figure 8

Multi-isotopic (Li-B-Sr) characterization of geothermal waters from the Taupo Volcanic Zone.

667 Figure 1

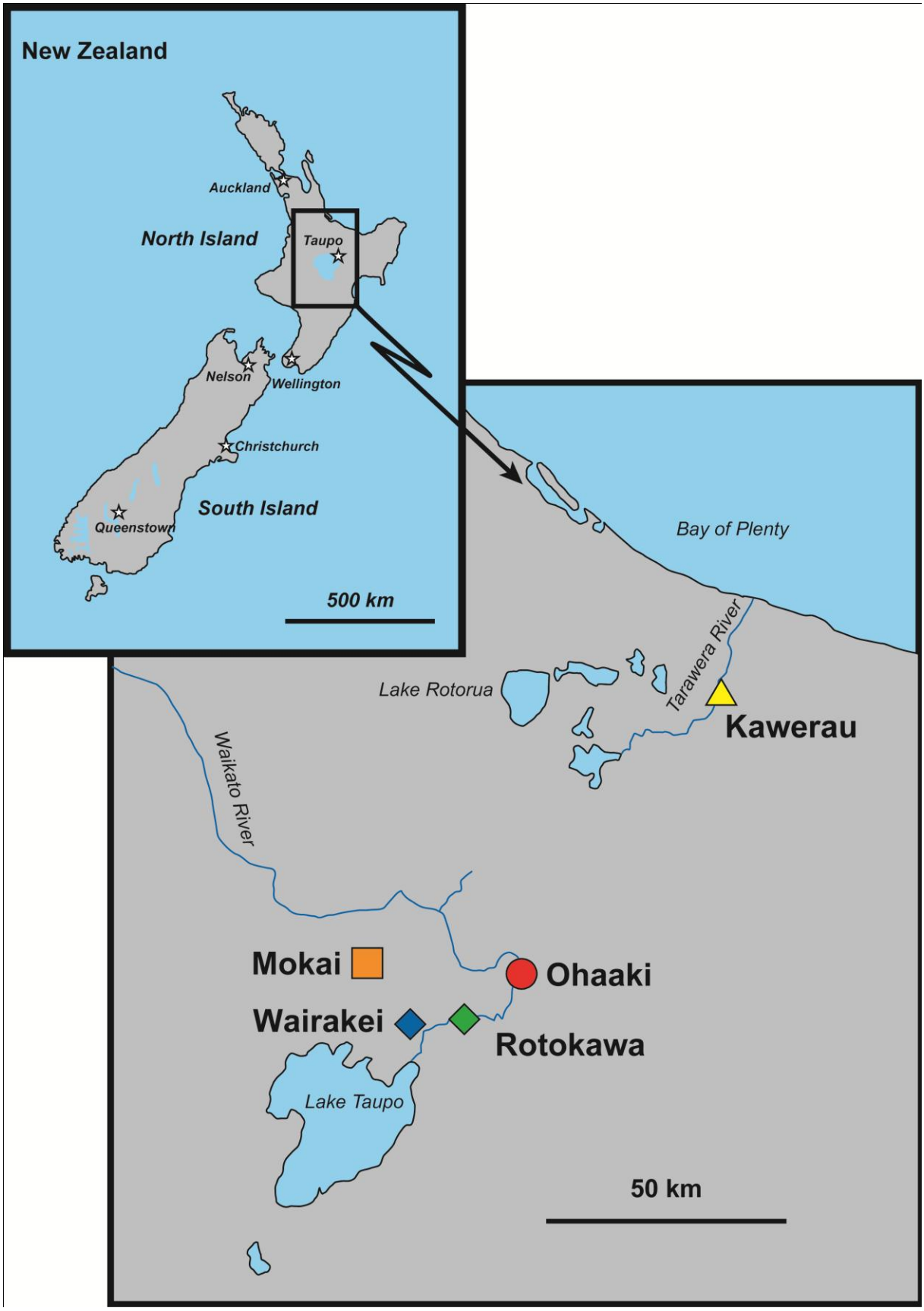

668

669

Figure 2

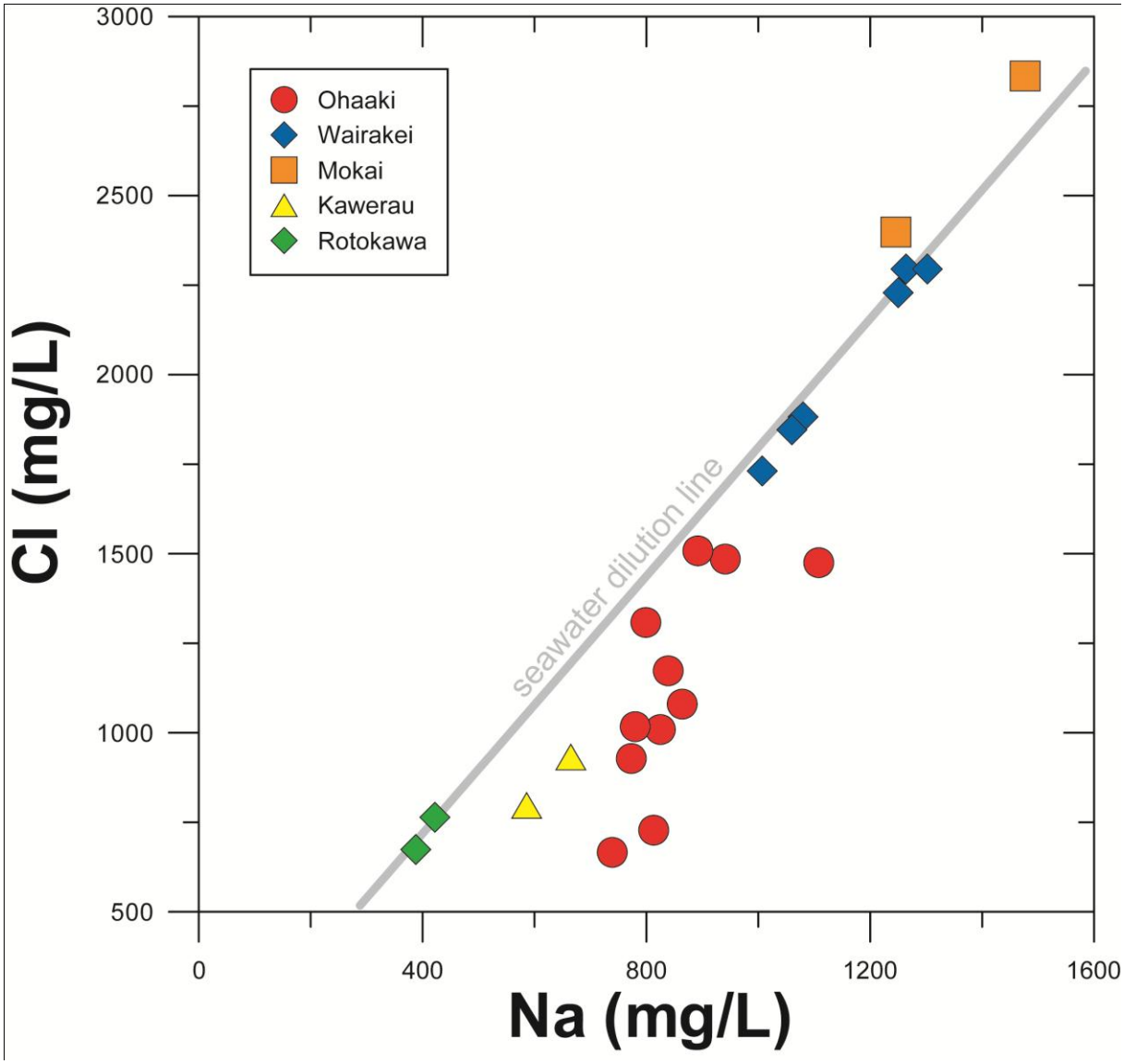
Ohaaki
Wairakei
Mokai
Kawerau
Rotokawa
seawater dilution line
Cl (mg/L)
Na (mg/L)
3000
2500
2000
1500
1000
500
0
400
800
1200
1600

685 Figure 3

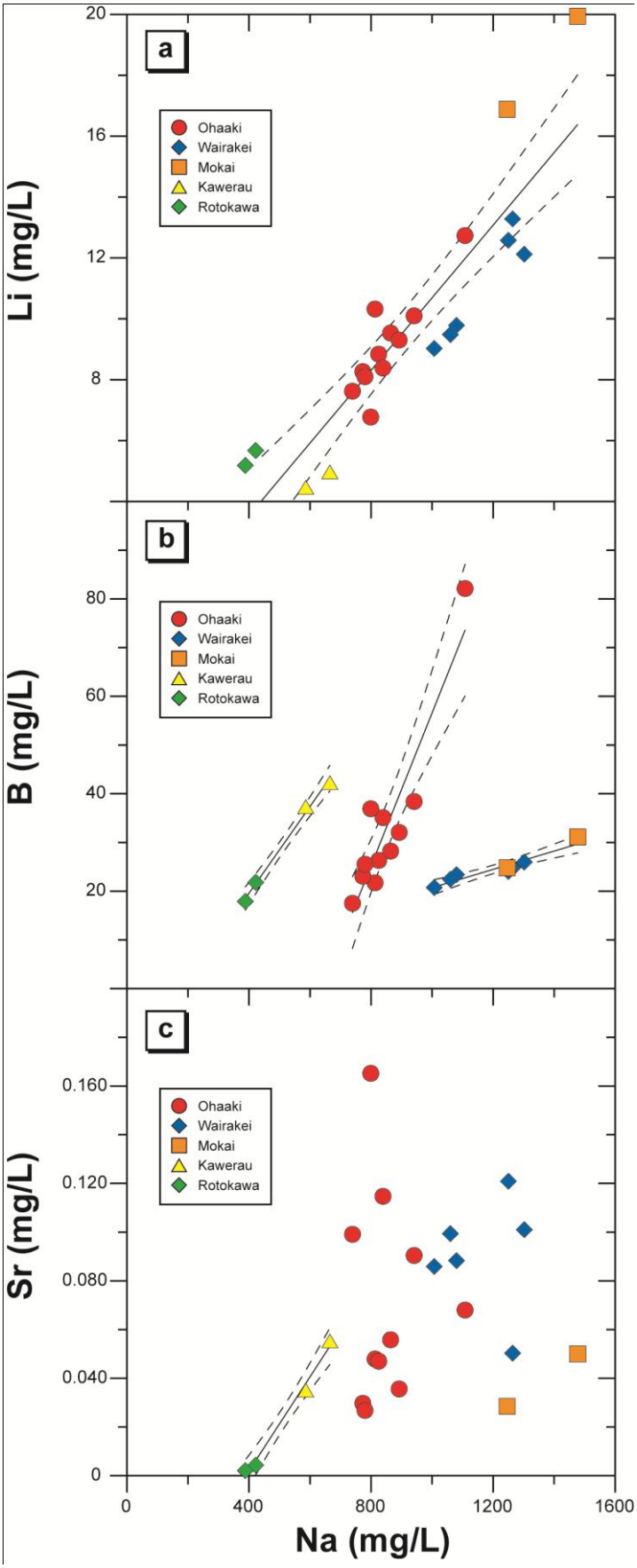

686

687

Figure 4

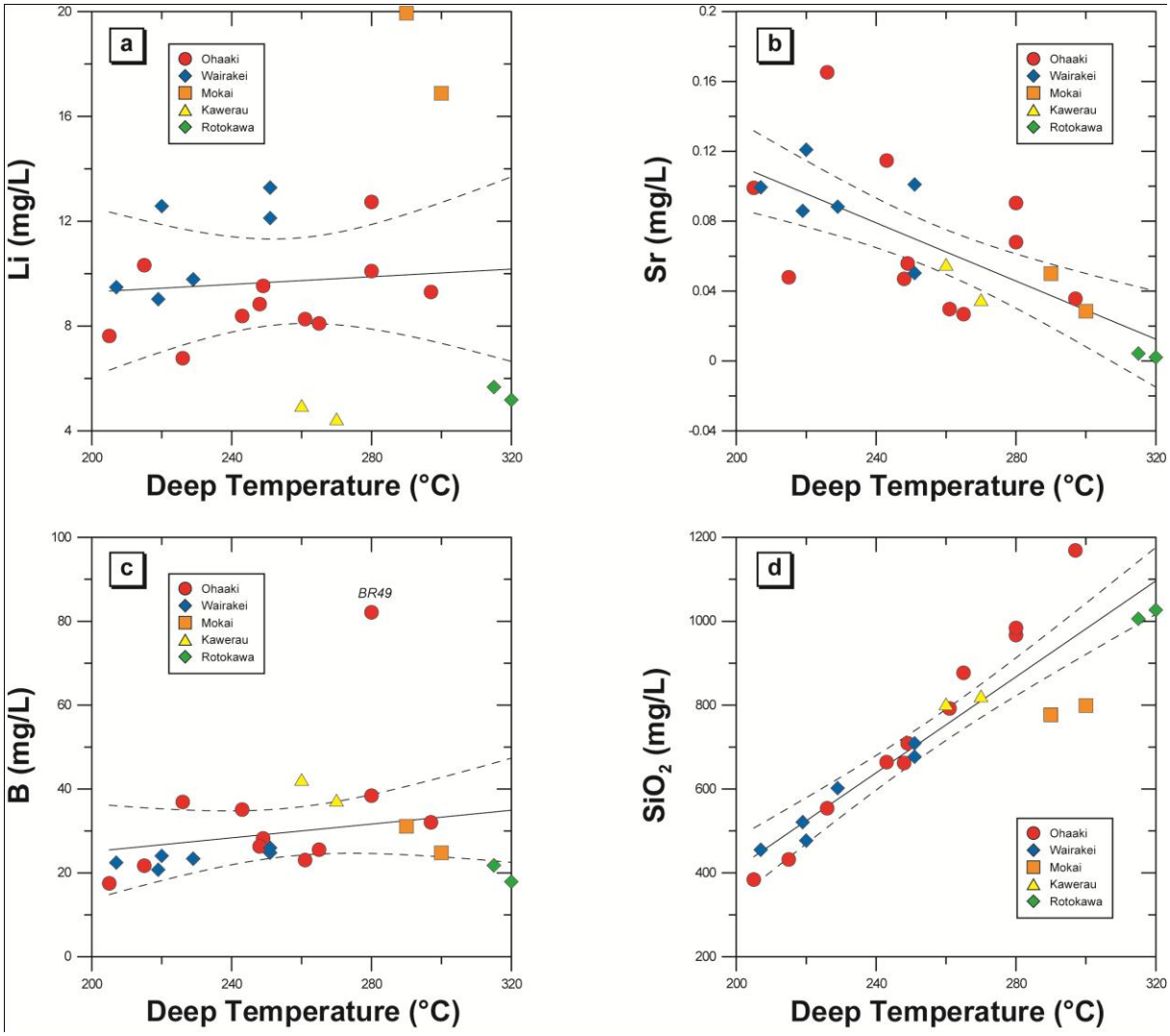
a
Ohaaki
Wairakei
Mokai
Kawerau
Rotokawa
Li (mg/L)
Deep Temperature (°C)
b
Sr (mg/L)
Deep Temperature (°C)
c
BR49
B (mg/L)
Deep Temperature (°C)
d
SiO2 (mg/L)
Deep Temperature (°C)

704 Figure 5

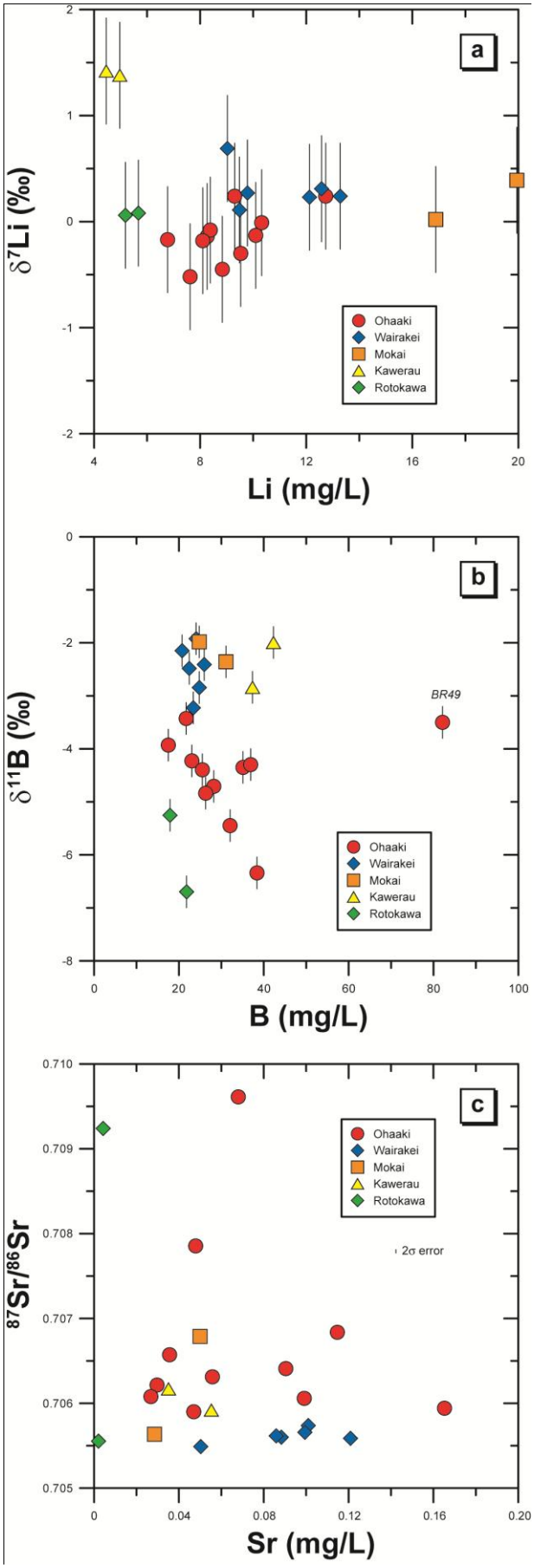

705

Figure 6

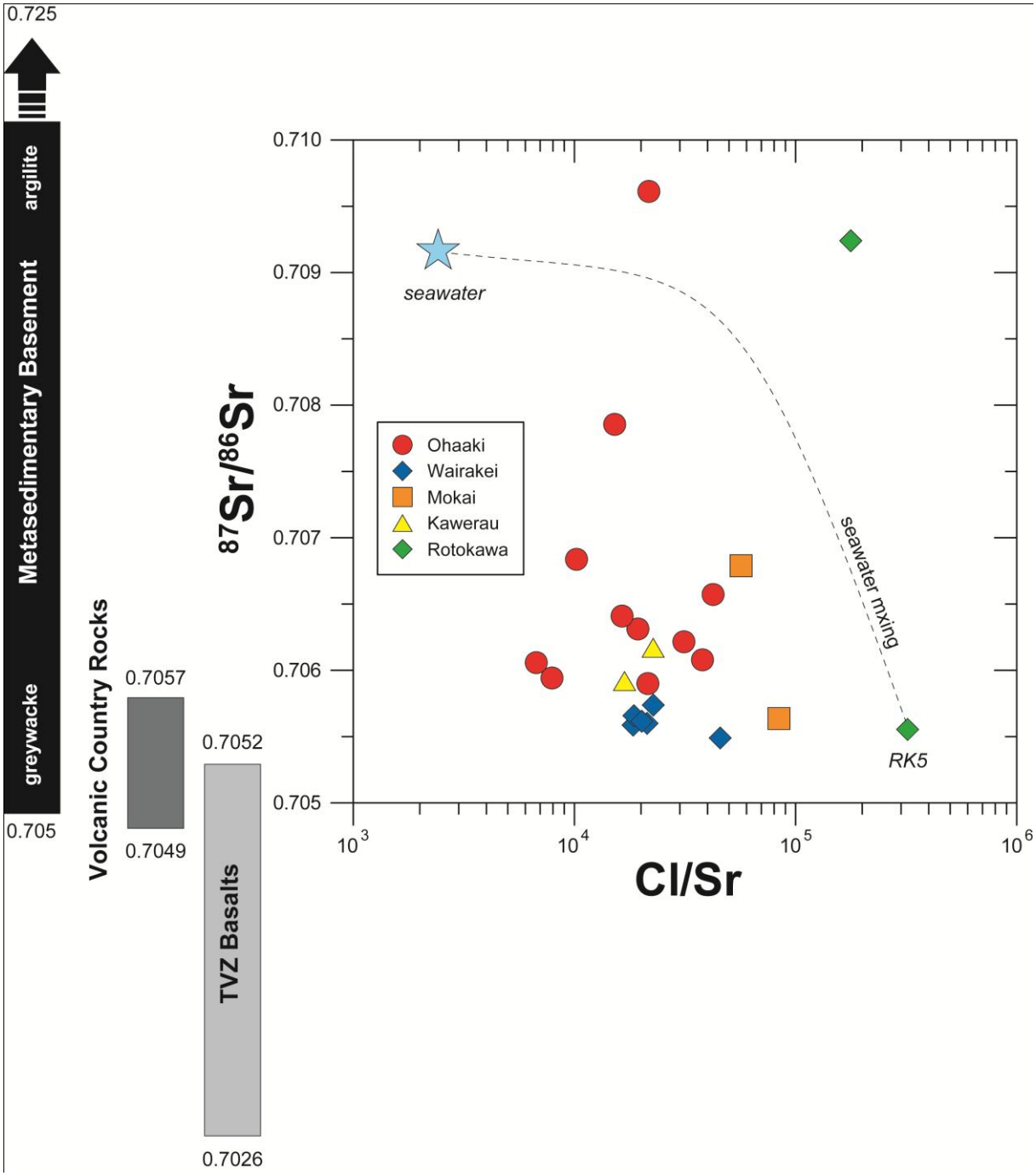
0.725
argilite
Metasedimentary Basement
greywacke
0.705
Volcanic Country Rocks
0.7057
0.7049
0.7052
TVZ Basalts
0.7026
0.710
0.709
0.708
0.707
0.706
0.705
87Sr/86Sr
seawater
seawater mixing
RK5
Ohaaki
Wairakei
Mokai
Kawerau
Rotokawa
10 3
10 4
10 5
10 6
Cl/Sr

716 Figure 7

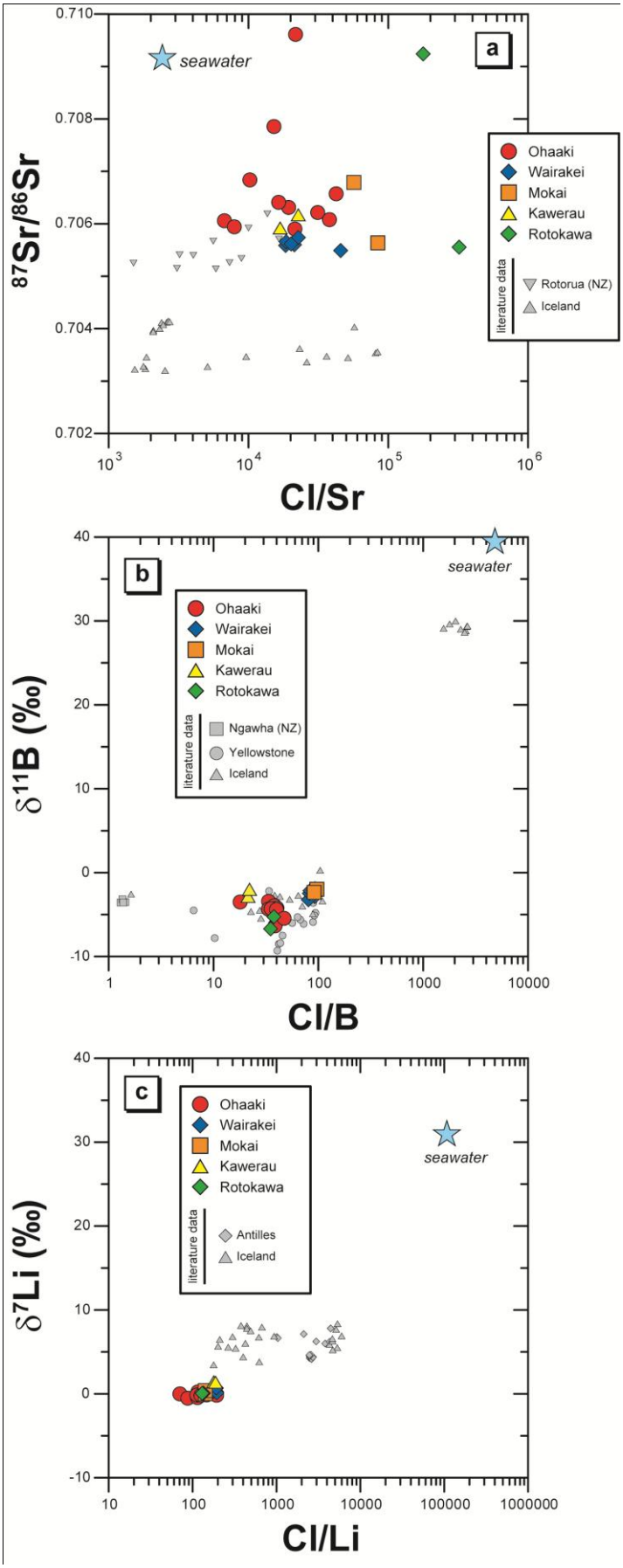

717

Figure 8

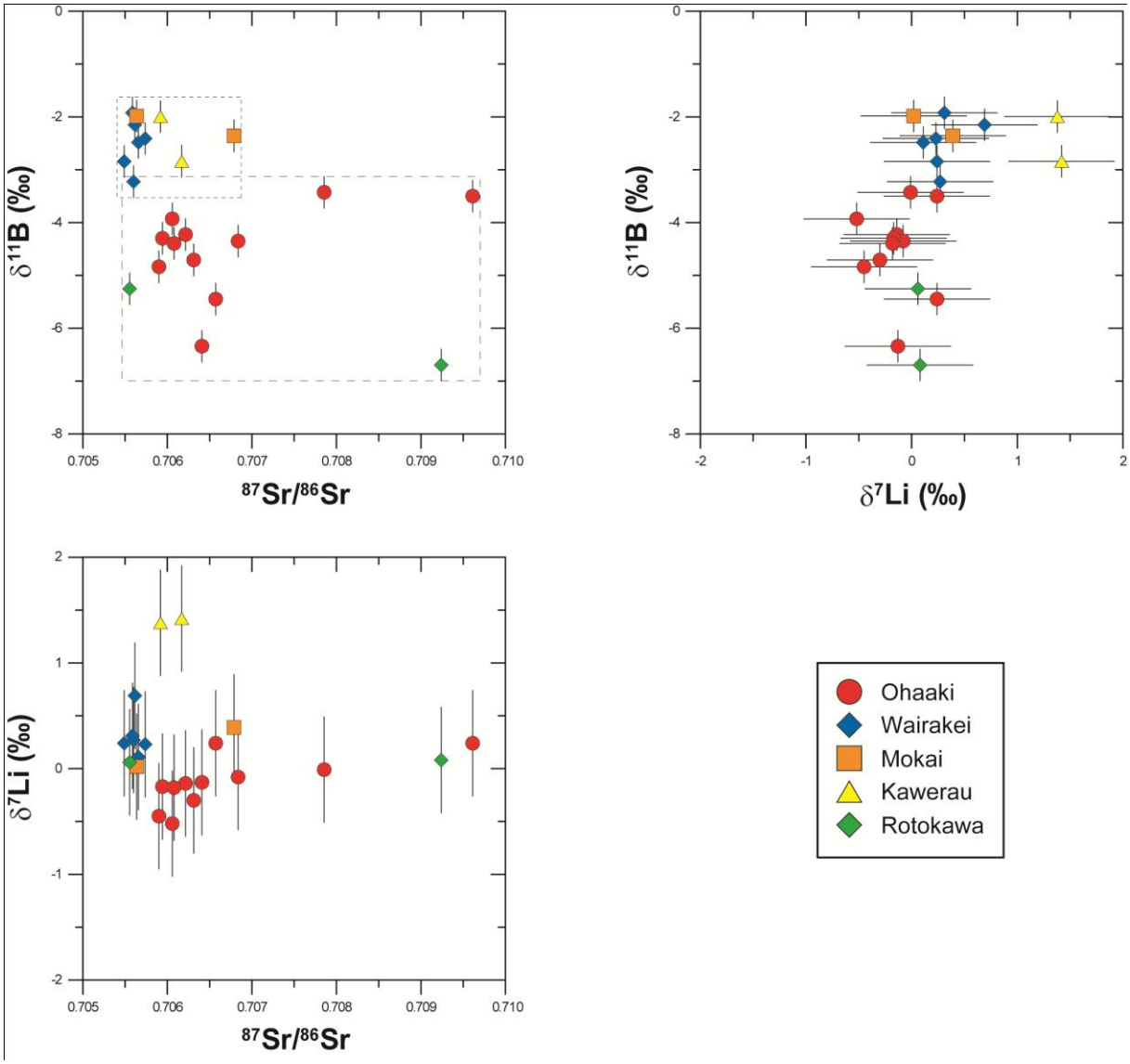
δ11B (‰)
87Sr/86Sr
δ7Li (‰)
δ11B (‰)
δ7Li (‰)
87Sr/86Sr
Ohaaki
Wairakei
Mokai
Kawerau
Rotokawa

733 Table 1

Geothermal system	Well ID	Coordinates		borehole depth	deep temperature	DATE	Na	K	Mg	Ca	Cl	SO_4	Br	SiO_2	Li	B	Sr	δ^7Li	$2\sigma_m$	δ^{11}B	$2\sigma_m$	$^{87}Sr/^{86}Sr$	$2\sigma_m$
		latitude	longitude	m	°C		mg/L	mg/L	µg/L	mg/L	mg/L	mg/L	mg/L	mg/L	mg/L	mg/L	µg/l	‰		‰			
Ohaaki	BR25	S 38°31'58"	E 176°18'43"	680	215	07/10/2004	813	94	< d.l.	0.106	728	19	2	432	10.32	21.71	47.9	-0.01	0.12	-3.43	0.09	0.707855	0.000006
Ohaaki	BR49	S 38°32'16"	E 176°18'37"	1270	280	04/10/2005	1108	206.5	8.4	2.143	1475	4	3.7	967	12.74	82.13	68	0.24	0.16	-3.50	0.08	0.709612	0.000006
Ohaaki	BR9	S 38°31'11"	E 176°18'24"	1000	205	03/04/2006	739	72.2	8.3	1.647	666	74.8	1.9	384	7.62	17.50	99.1	-0.52	0.14	-3.93	0.06	0.706058	0.000009
Ohaaki	BR22	S 38°31'10"	E 176°18'34"	670	249	03/04/2006	864	137.4	5.3	1.758	1080	58.8	3.1	709	9.53	28.22	55.8	-0.30	0.24	-4.71	0.07	0.706312	0.000007
Ohaaki	BR20	S 38°31'18"	E 176°18'36"	1000	248	23/04/2007	825	110.2	15.4	1.859	1009	60.5	3	662	8.84	26.31	47	-0.45	0.22	-4.84	0.08	0.705900	0.000007
Ohaaki	BR54	S 38°31'06"	E 176°18'35"	1430	261	01/05/2007	773	121.4	< d.l.	1.624	928	43.5	2.7	792	8.27	23.06	29.7	-0.14	0.20	-4.23	0.11	0.706215	0.000007
Ohaaki	BR44	S 38°31'53"	E 176°19'06"	760	243	28/08/2007	839	102.2	5.1	2.146	1173	12.4	3.2	664	8.38	35.10	114.7	-0.08	0.18	-4.35	0.09	0.706837	0.000007
Ohaaki	BR14	S 38°37'06"	E 176°19'19"	590	226	31/08/2007	799	81.1	25.4	12.625	1308	3.9	3.7	554	6.77	36.91	165.2	-0.17	0.24	-4.30	0.07	0.705942	0.000007
Ohaaki	BR48	S 38°31'06"	E 176°17'53"	1360	265	28/09/2007	780	136.1	< d.l.	1.872	1017	41.3	2.8	877	8.10	25.53	26.8	-0.18	0.12	-4.39	0.07	0.706079	0.000007
Ohaaki	BR60	S 38°31'10"	E 176°17'54"	1800	280	23/07/2008	941	199.2	8.9	2.686	1485	10.2	4.4	984	10.10	38.40	90.4	-0.13	0.10	-6.34	0.07	0.706409	0.000008
Ohaaki	BR56	S 38°31'01"	E 176°18'17"	1880	297	03/09/2008	892	220.5	27.9	3.003	1508	9.5	4.3	1169	9.30	32.06	35.6	0.24	0.26	-5.45	0.08	0.706572	0.000006
Wairakei	WK245	S 38°37'04"	E 176°02'59"	800	251	07/09/2008	1264	217.4	< d.l.	10.923	2295	34.1	5.4	709	13.28	24.81	50.3	0.24	0.14	-2.84	0.09	0.705490	0.000009
Wairakei	WK70	S 38°37'22"	E 176°04'22"	600	229	08/10/2008	1080	146.1	8.6	20.434	1882	35	4.5	602	9.78	23.39	88.3	0.27	0.30	-3.23	0.08	0.705600	0.000008
Wairakei	WK247	S 38°36'55"	E 176°03'20"	2300	251	05/03/2007	1302	213.2	7.5	27.667	2295	34	5.8	677	12.12	25.97	101	0.23	0.12	-2.41	0.09	0.705738	0.000007
Wairakei	WK235	S 38°36'53"	E 176°03'23"	700	220	04/03/2008	1250	175.6	9.2	20.911	2229	33.7	5.6	477	12.58	24.06	120.9	0.31	0.18	-1.92	0.09	0.705587	0.000008
Wairakei	WK28	S 38°37'32"	E 176°04'09"	600	207	14/04/2008	1060	139.3	16.7	21.261	1846	44.4	4.6	455	9.48	22.44	99.4	0.11	0.18	-2.48	0.12	0.705658	0.000008
Wairakei	WK24	S 38°37'21"	E 176°04'18"	600	219	30/07/2008	1007	128.2	7.2	20.247	1731	34.9	4.3	521	9.03	20.75	85.9	0.69	0.18	-2.15	0.08	0.705616	0.000007
Mokai	MK3	S 38°31'34"	E 175°56'23"	1679	300	24/02/2009	1246	288.6	14.6	7.965	2398	11.7	5.6	799	16.88	24.79	28.5	0.02	0.16	-1.98	0.09	0.705636	0.000006
Mokai	MK7	S 38°31'36"	E 175°55'34"	2252	290	25/02/2009	1477	338.2	27.2	12.086	2834	6.6	5.9	777	19.94	31.10	50	0.39	0.16	-2.36	0.09	0.706789	0.000007
Kawerau	KA37	S 38°03'52"	E 176°43'34"	1306	270	29/01/2009	586	92.9	< d.l.	1.891	797	26.4	2	822	4.46	37.34	35.1	1.42	0.18	-2.84	0.06	0.706170	0.000009
Kawerau	KA19	S 38°03'32"	E 176°43'07"	1108	260	28/01/2009	665	99.4	6.9	2.468	932	14.6	2	803	4.97	42.28	55.3	1.38	0.16	-1.99	0.06	0.705919	0.000007
Rotokawa	RK14	S 38°36'33"	E 176°11'25"	2500	315	08/04/2009	422	126.7	< d.l.	1.632	764	2.6	1.3	1006	5.67	21.80	4.3	0.08	0.16	-6.70	0.06	0.709240	0.000007
Rotokawa	RK5	S 38°36'31"	E 176°11'40"	2783	320	07/04/2009	388	112.1	< d.l.	1.232	674	3.9	1.1	1027	5.18	17.90	2.1	0.06	0.20	-5.25	0.07	0.705554	0.000007

734

735